Applications of the Fourier transform to the processing of vibration signals

Rainer, J. H.

Publisher's version / Version de l'éditeur:
https://doi.org/10.4224/40000474
Building Research Note, 1986-03

National Research Council Canada
Conseil national de recherches Canada

Institute for Research in Construction
Institut de recherche en construction

Building Research Note

Applications of the Fourier Transform to the Processing of Vibration Signals

by J.H. Rainer

BRN 233

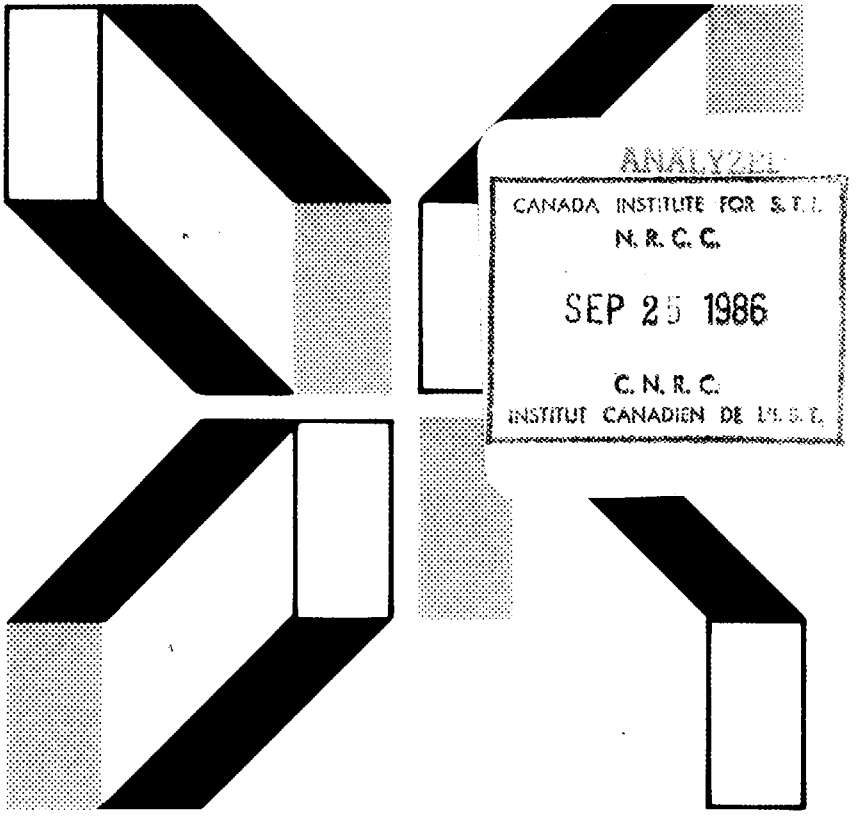

Canada

APPLICATIONS OF THE FOURIER TRANSFORM TO THE PROCESSING OF VIBRATION SIGNALS

by J.H. Rainer
Noise and Vibration Section
Institute for Research in Construction

BRN 233
ISSN 0701-5232
Ottawa, March 1986

TABLE OF CONTENTS

ABSTRACT

A number of operations for processing deterministic signals obtained from measurements of structural dynamics have been carried out in the frequency domain. They include instrument correction including angular motion, integration and differentiation, baseline adjustment, and filtering. A survey of computational considerations includes aliasing, the Fast Fourier Transform (FFT), the transformation of long records, wrap-around, and the leakage phenomenon. Numerical examples illustrate baseline adjustment, leakage, and wrap-around.

RÉSUMÉ

L'auteur a effectué un certain nombre d'opérations, dans le domaine des fréquences, en vue de traiter les signaux déterministes obtenus à partir de mesures de dynamique structurale : correction instrument pour tenir compte du mouvement angulaire, intégration et différenciation, ajustement des valeurs de référence et filtrage. Il passe en revue certains paramètres de calcul comme l'aliasing, la transformation rapide de Fourier (TRF), la transformation des longs enregistrements, le bouclage et le phénomène de fuite. Il donne des exemples numériques d'ajustement des valeurs de référence, de fuite et de bouclage.

INTRODUCTION

Signals obtained from measurements in structural dynamics (and other disciplines) need to be processed before they can be used in interpreting the behaviour of the object under investigation. Such processing may include instrument correction, integration and differentiation, filtering, and consideration of other influences on transducer behaviour such as angular motion that accompanies horizontal movement of slender structures. This applies to signals from both laboratory tests and full-scale field observations. The latter are more likely to require some of the above operations since the experimental conditions are not always under the full control of the investigator; some effects are also more pronounced at the low frequencies that pertain to the motions of large structures.

The traditional method of processing signals from transducers has been in the time domain using digital or analog methods. With the advent of the efficient computation scheme of the Fast Fourier Transform (FFT), processing in the frequency domain has become a practical reality. The frequency domain not only provides a viable alternative to time domain methods, but permits the solution of problems that involve frequency dependent parameters.

This report discusses the application of some common methods of processing signals from structural dynamics in the deterministic sense. Probabilistic or statistical procedures such as signal averaging and probability distributions are not discussed here. Although some aspects of the following operations are well known, they are included here to provide the necessary background to new procedures such as baseline correction and instrument correction for angular motion.

THE FOURIER TRANSFORM METHOD

The Fourier transform method as it applies to structural dynamics will be reviewed only briefly since numerous books deal with this subject in detail [1-4]. The Discrete Fourier Transform (DFT) of the discrete series $x(k\Delta t)$, consisting of N points of uniform spacing Δt, is:

$$X(n\Delta f) = \sum_{k=0}^{N-1} x(k\Delta t) e^{-j2\pi nk/N} \tag{1}$$

for $n = 0, 1, \ldots N-1$; the inverse Fourier transform is:

$$y(k\Delta t) = \sum_{n=0}^{N-1} Y(n\Delta f) e^{j2\pi nk/N} \tag{2}$$

for $k = 0, 1, \ldots N-1$; $j = \sqrt{-1}$.

The DFT corresponds to the integral form of the Fourier transform at the discrete points, provided that the signal is fully within the range of summation, and the frequency content is less than half the Nyquist frequency (f_m) [2,4].

The response of a linear system with impulse response function $h(t)$ when subjected to a disturbance $x(t)$ is given by the convolution integral, also called the Duhamel integral:

$$y(t) = \int_{-\infty}^{t} x(\tau)\ h(t-\tau)d\tau. \tag{3}$$

This convolution is commonly written as:

$$y(t) = x(t) * h(t). \tag{4}$$

Taking the Fourier transform throughout Eqs. (3) or (4) gives:

$$Y(\omega) = X(\omega)\ H(\omega) \tag{5}$$

where $H(\omega)$, called the frequency response function, is the Fourier transform of the impulse response function $h(t)$, and $X(\omega)$ and $Y(\omega)$ are the Fourier transforms of $x(t)$ and $y(t)$, respectively. $H(\omega)$ is, in general, a complex function and can be obtained from the differential equation of motion, from the Fourier transform of the impulse response function $h(t)$, or by measuring the phase and amplitude response of the system to sinusoidal inputs. Once the desired frequency response function of the system is known, the multiplication in Eq. (5) is carried out over the entire frequency range and the signal $y(t)$ is obtained by taking the inverse Fourier transform according to Eq. (2). An example of the computation of the response of a single-degree-of-freedom oscillator subjected to the El Centro 1940 N-S ground motion is given in Reference 5.

For calculating the DFT, the Fast Fourier Transform (FFT) algorithm [1,6] represents an efficient computational method. It requires, however, that the total number of discrete points N be an integer power of 2; i.e., $N = 2^n$. Where the available real points do not form a full 2^n values, zeros can be added. See References 1 and 6 for further details.

OPERATIONS ON DETERMINISTIC SIGNALS

Instrument Correction of Transducer Signals

The signal from the transducer represents the motion of the structure as modified by the instrument characteristics. That is, the transducer signal $y(t)$ can be viewed as the convolution of the structure motion $x(t)$ by the transducer characteristic $h(t)$, as given by Eq. (4) in the time domain or Eq. (5) in the frequency domain. In order to obtain the true structural motion $x(t)$, it is necessary to apply an instrument correction, in which

the transducer signal is "deconvolved" by the instrument characteristics. In the frequency domain, this becomes:

$$X(\omega) = \frac{1}{H(\omega)} Y(\omega). \tag{6}$$

The frequency response function $H(\omega)$ for a transducer that is modelled by a spring-mass oscillator can be obtained from the differential equation of motion:

$$\ddot{u} + 2\beta\omega_0\dot{u} + {\omega_0}^2 u = -\ddot{x}(t) \tag{7}$$

where:

u = displacement of mass relative to transducer base,
ω_0 = natural frequency of the transducer (rad/s),
β = critical damping ratio of the transducer,
$x(t)$ = base motion,

and dots refer to differentiation with respect to time.

Assuming a base motion $x(t) = Ae^{j\omega t}$ and response $u(t) = Be^{(j\omega t+\psi)}$, the frequency response function is the ratio of relative output displacement u to the input displacement x:

$$H(\omega) = \frac{\Omega^2}{1 - \Omega^2 + j2\beta\Omega} \tag{8}$$

where the frequency ratio $\Omega = \frac{\omega}{\omega_0}$. Thus for a transducer that is closely modelled by a single-degree-of-freedom oscillator, it is only necessary to know its natural frequency and damping ratio, and the correction function can be obtained by Eq. (8). Complex multiplication with the Fourier-transformed signal $y(t)$ according to Eq. (5), and application of the inverse Fourier transform gives the instrument-corrected signal, $x(t)$.

The instrument correction can be carried through and beyond the resonance frequency of the transducer and thereby frequency components can be restored which were attenuated due to inadequate transducer response. This correction procedure also restores the original phase relationships among the signal components. Although such instrument correction is not always necessary, it becomes important for impulsive types of loading and for processing of strong-motion seismograph signals when the frequency content of the signal is near the natural frequency of the transducer.

Instrument Correction Including Angular Motion

When angular motion is present simultaneously with horizontal movement, the signal from a transducer placed to respond in the horizontal direction will be affected by this rotation.

Transducers on tall slender structures such as towers and chimneys, and long slender cable structures such as suspension bridges are particularly prone to this effect.

The frequency response function for relative displacement of the transducer mass when subjected to a base displacement and angular motion is [7]:

$$H(f) = \frac{\Omega^2 + \frac{g}{R\omega_0{}^2}}{1 - \Omega^2 + j2\beta\Omega} \tag{9}$$

where:

g = acceleration due to gravity,
R = radius of rotation of transducer base,
ω_0 = natural frequency of instrument (rad/s).

The complex division of $Y(\omega)$ by $H(\omega)$, as indicated by Eq. (6), and the inverse Fourier transform, gives the actual horizontal motion of the structure, $x(t)$.

Further details of rotation correction procedures and numerical examples are presented in References 7 and 8.

Filtering

Filtering is removal of specific ranges of frequency components from a signal. This can be achieved numerically or by analog methods in the time domain, or by computing the Fourier transform, deleting undesired frequency components, and then calculating the inverse Fourier transform to obtain the filtered time signal. Specifically, if $H(\omega)$ is a function having the desired filter shape in the frequency domain (a 'frequency window'), taking the product with the transform of the signal, as in Eq. (5), and the inverse Fourier transform, as in Eq. (2), yields the desired filtered signal. Representative window shapes in the time and frequency domains are shown in Figure 1. Aspects of leakage need to be considered, however; these are discussed in another section.

A useful property of the filtering described above is that the phase relationships of the frequency components of the signal are not changed, which is not the case for analogue filters. The mean and other boundary conditions may change, however, so that a baseline adjustment may be necessary for every filtering operation. Baseline adjustment will be discussed below.

Differentiation and Integration

Differentiation and integration in the frequency domain correspond to multiplication of the appropriate function of $j\omega$, since:

$$\frac{d}{dt}(e^{j\omega t}) = j\omega e^{j\omega t}. \tag{10}$$

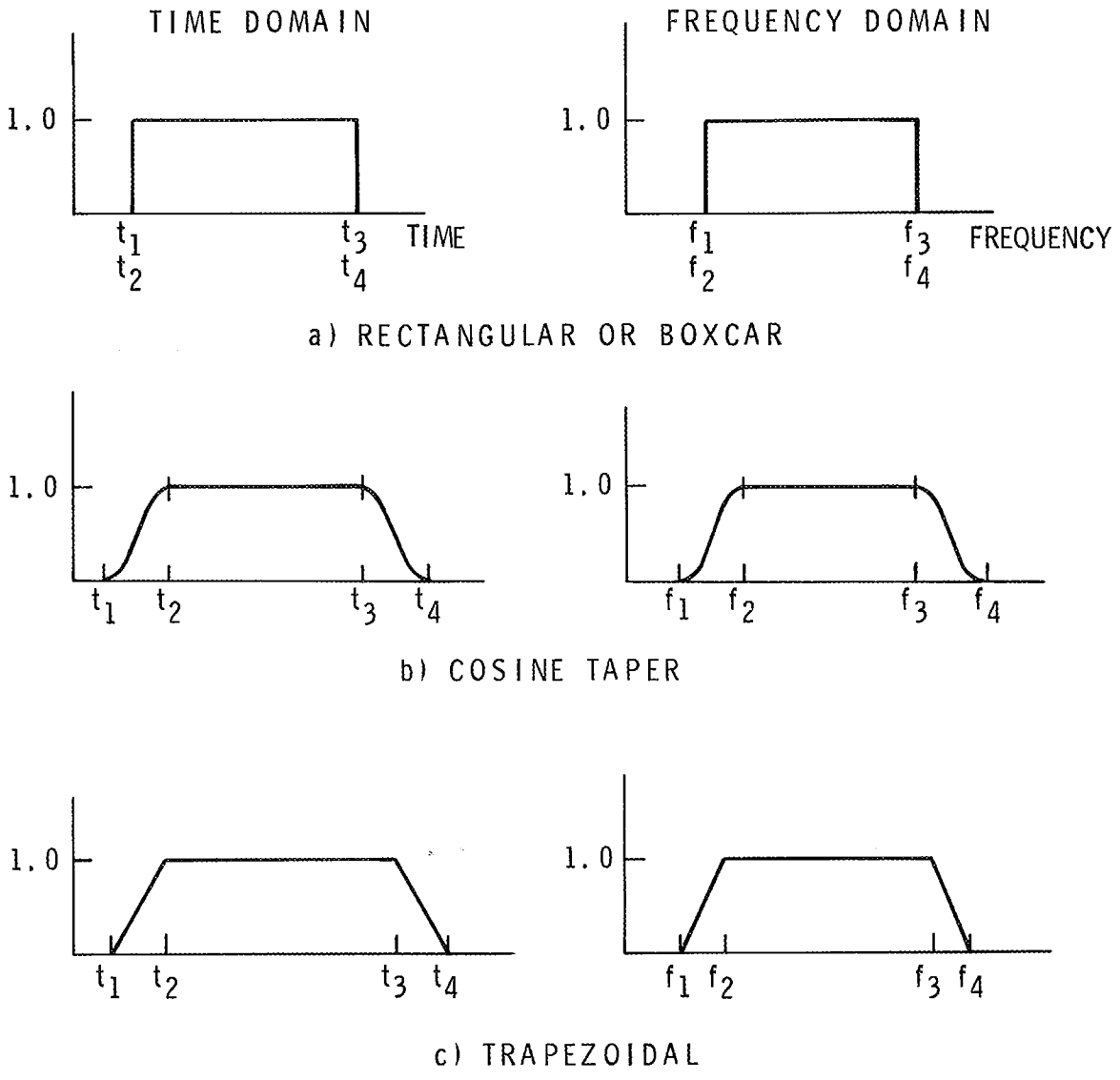

Figure 1 Some common time and frequency windows.

Thus for differentiation, the applicable frequency response function is:

$$H(\omega) = j\omega. \tag{11}$$

For double differentiation, the frequency response function is the product for two single differentiations:

$$H(\omega) = -\omega^2. \tag{12}$$

Similarly, for single or double integration:

$$H(\omega) = \frac{1}{j\omega} \tag{13}$$

$$H(\omega) = \frac{1}{-\omega^2}. \tag{14}$$

Here, $\omega = 2\pi f$, where f is the circular frequency in Hz. After multiplication throughout the frequency range, as indicated by Eq. (5), the inverse transform then yields the integrated or differentiated signal $y(t)$.

In performing the integration, ω or $f = 0$ cannot be admitted, since the result of the division by zero would yield ∞. This is resolved by setting the first term in the frequency domain equal to zero, which results in a signal with zero mean, as will be discussed below.

Baseline Adjustment

Baseline adjustment becomes necessary when the signal or some function of it needs to satisfy certain boundary conditions, which can include zero initial and final values, zero mean, or zero final value of the integral of the signal. The required baseline adjustments have commonly been carried out in the time domain and are incorporated into widely accepted methods of processing strong-motion seismograph records [9]. Many of such boundary conditions can also be achieved by specifying the necessary conditions in the frequency domain [10,11]. The simplest such form of baseline adjustment is the requirement for zero mean value. Examination of Eq. (1) shows that the term corresponding to $f = 0$ or $n = 0$ represents the sum of all the signal amplitudes, which is the mean value times the signal length. Consequently, with the zero'th term set to zero, the signal will have a baseline correction that corresponds to zero mean value.

In a more general case, based on physical considerations of elastic behaviour, the following boundary conditions may need to be satisfied by a ground motion record obtained from blasting or seismic activity:

1) zero mean acceleration, velocity and displacement;
2) zero beginning and final velocity;
3) zero beginning and final displacement.

For the FFT to be employed in the analysis of a record, $N = 2^n$ points are required. For record length of k points less than N, the signal thus has two parts: 1) the actual record up to time t_k; and 2) the augmented portion of zeros up to time t_N (Fig. 2a). Since the augmented record is the more general case, it will be treated here in detail. The boundary conditions listed above need to be satisfied for the actual portion of the record up to t_k, as well as for the entire signal used for computation up to time t_N.

The baseline adjustment of the acceleration record is carried out in two stages, satisfying in turn the boundary conditions for both the velocity and the displacement. The procedure is illustrated on a recorded acceleration ground motion from a distant excavation blast, shown in Figure 2 along with unadjusted integrated velocities and displacements. The acceleration record has been adjusted for instrument characteristics and the integrations are carried out in the frequency domain according to the methods described above.

Velocity boundary conditions Since the start and finish of the velocity up to time t_k is to be equal (and eventually zero), an angular baseline shift from the starting value v_0 at time $t_0 = 0$ to the finishing value v_k at time t_k, has to be made. This corresponds to a constant adjustment to the acceleration trace:

$$\Delta \underline{a} = \frac{v_0 - v_k}{t_k}. \tag{15}$$

The resulting acceleration trace is shown in Figure 3a and the corresponding velocity trace in Figure 3b. The acceleration trace is virtually indistinguishable from that of the uncorrected trace in Figure 2a because the correction is so small, but it is included here and in subsequent correction stages for completeness and for comparison purposes.

Now a constant shift $\bar{v}$ on the velocity trace is performed to bring the start and finish to zero. In order to maintain the zero mean velocity, a parabola that has the same area as the rectangle formed by the total time t_N multiplied by the amount of adjustment $\bar{v}$ is subtracted from the actual velocity record of duration t_k.

The area of the correction parabola is $\frac{2}{3} y_c t_k$, where y_c is the centre amplitude of the parabola, and this is equal to $\bar{v} t_k$, the area of rectangle up to time t_k; thus:

$$y_c = \frac{3}{2}\bar{v}. \tag{16}$$

From geometry, the equation of the parabola that corrects the velocity curve is then:

$$\Delta w(t) = \frac{6\bar{v}}{t_k^2}\left(t - \frac{t_k}{2}\right)^2. \tag{17}$$

Since the acceleration represents the derivative of the velocity with respect to time, the acceleration adjustment is:

$$\Delta \dot{w}(t) = \frac{12\bar{v}}{t_k^2}\left(t - \frac{t_k}{2}\right). \tag{18}$$

However, the total area of the rectangle to be corrected in the computation is $\bar{v} t_N$, so that the correction term has to be multiplied by t_N / t_k:

$$\Delta \underline{\dot{w}}(t) = \frac{12\bar{v}}{t_k^2}\left(t - \frac{t_k}{2}\right) t_N / t_k. \tag{19}$$

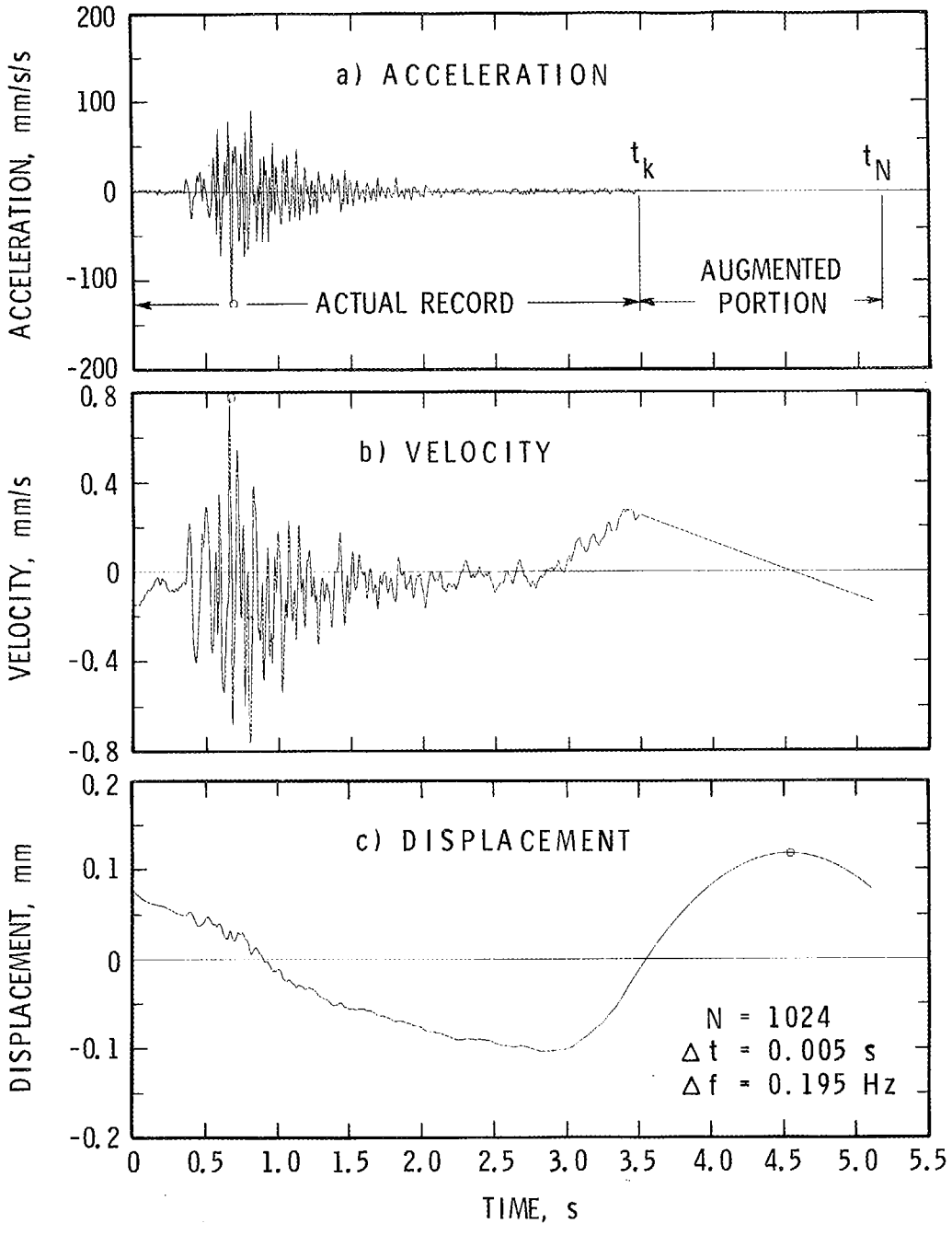

Figure 2 Unadjusted acceleration record and resulting velocity and displacement.

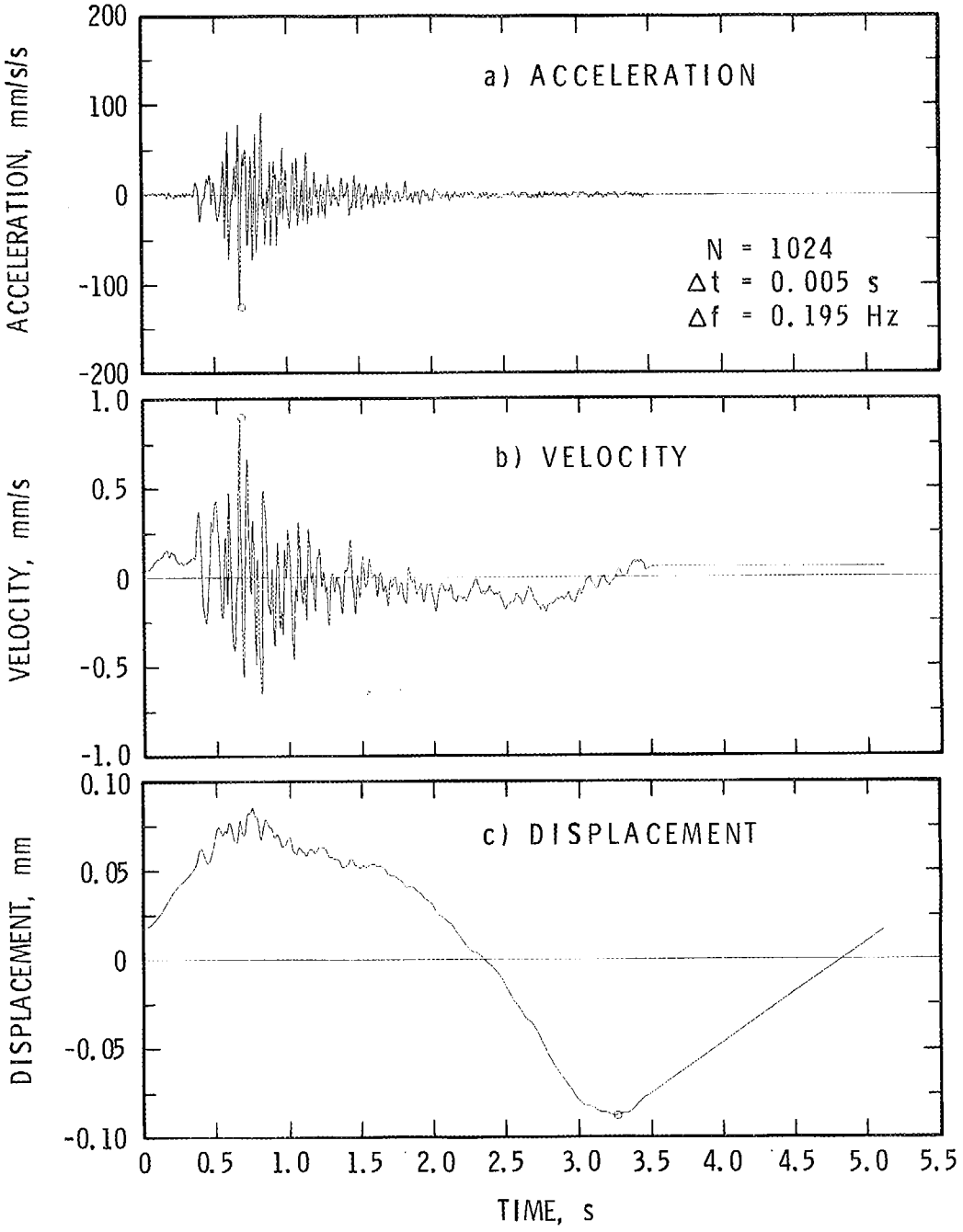

Figure 3 Acceleration record adjusted by constant $\bar{v}$ and resulting velocity and displacement.

Thus the acceleration trace corrected to satisfy the velocity boundary conditions is:

$$\ddot{x}_v(t) = \ddot{x}(t) - \underline{a} - \Delta\underline{\dot{w}}(t). \tag{20}$$

The velocity-corrected acceleration trace is shown in Figure 4a and the resulting velocity and displacements in Figures 4b and c, respectively. Again, this acceleration trace is virtually indistinguishable from the uncorrected one in Figure 2a.

Displacement boundary conditions The displacement that results from the acceleration record $\ddot{x}_v$ adjusted for the velocity conditions is shown in Figure 4c. An adjustment similar to that for the velocity boundary condition is now applied in order to satisfy the boundary conditions of the displacement record. But here the adjustment function to the displacement trace needs to have a continuous slope or derivative at t_k, where it joins the augmented portion, in order not to result in a discontinuity in the corrected velocities or accelerations. Therefore the correction cannot be a second degree parabola. The simplest acceptable function is a third degree polynomial, or the trigonometric function with amplitude u:

$$\Delta z(t) = u \cos 2\pi t/t_k. \tag{21}$$

The corresponding derivatives are then:

$$\Delta\dot{z}(t) = (\frac{2\pi}{t_k})u \sin\ 2\pi t/t_k \tag{22}$$

$$\Delta\ddot{z}(t) = -(\frac{2\pi}{t_k})^2 u \cos\ 2\pi t/t_k. \tag{23}$$

Again, $\Delta\ddot{z}$ has to be multiplied by the ratio t_N/t_k to compensate for the portion of the correction rectangle in the region with the added zeros. Thus:

$$\Delta\underline{\ddot{z}}(t) = -(\frac{t_N}{t_k})(\frac{2\pi}{t_k})^2 u \cos 2\pi t/t_k \tag{24}$$

and the acceleration record corrected for both the velocity and displacement boundary conditions becomes:

$$\ddot{x}_d(t) = \ddot{x}(t) - \underline{a} - \Delta\underline{\dot{w}}(t) - \Delta\underline{\ddot{z}}(t). \tag{25}$$

The adjusted acceleration, resulting velocity, and displacement are shown in Figures 5a, b, and c, respectively.

The slight deviation from zero in the displacement trace in the extended region of the record is due to small numerical inaccuracies such as round-off errors and discretization

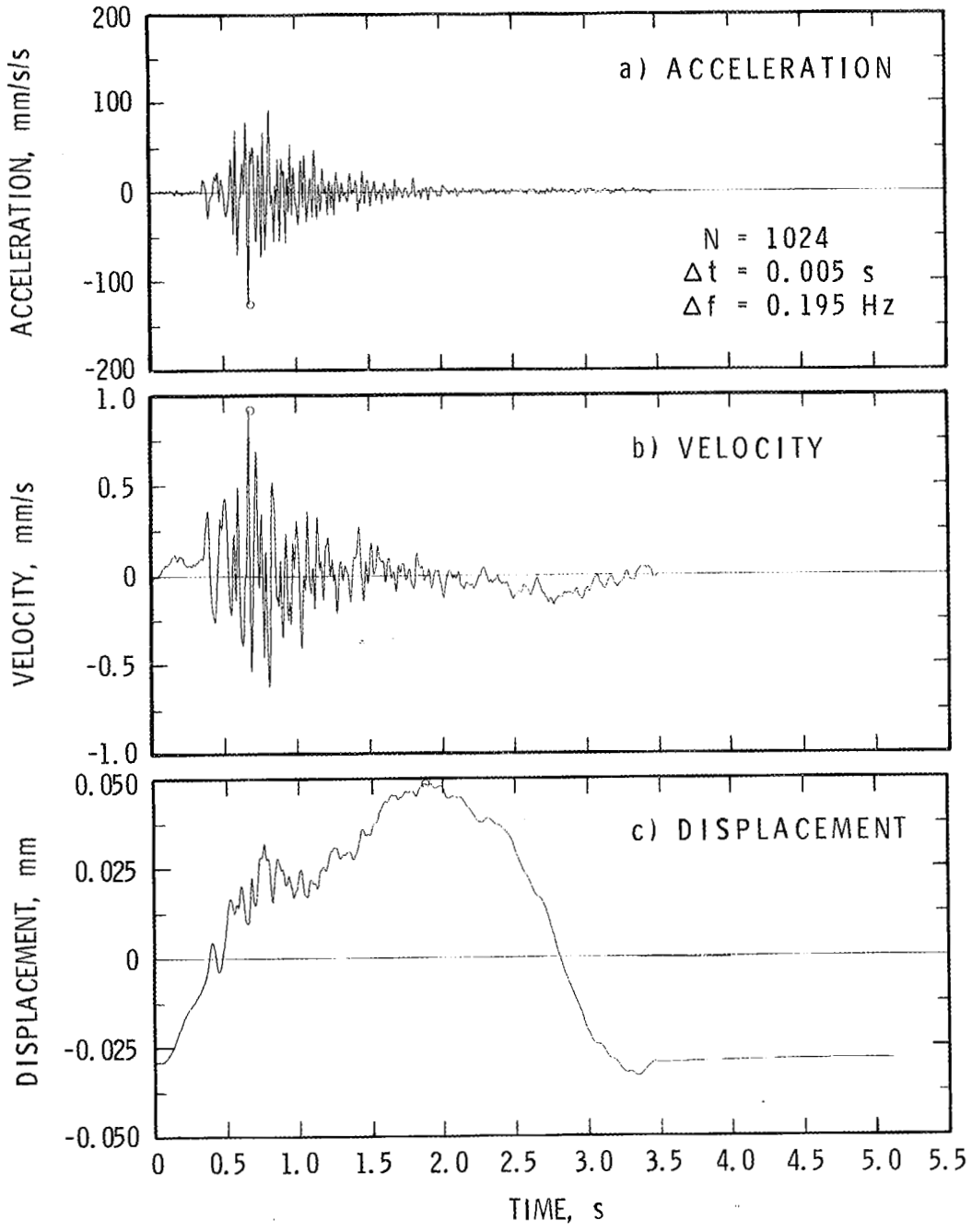

Figure 4 Acceleration signal adjusted for velocity boundary conditions and resulting velocity and displacement.

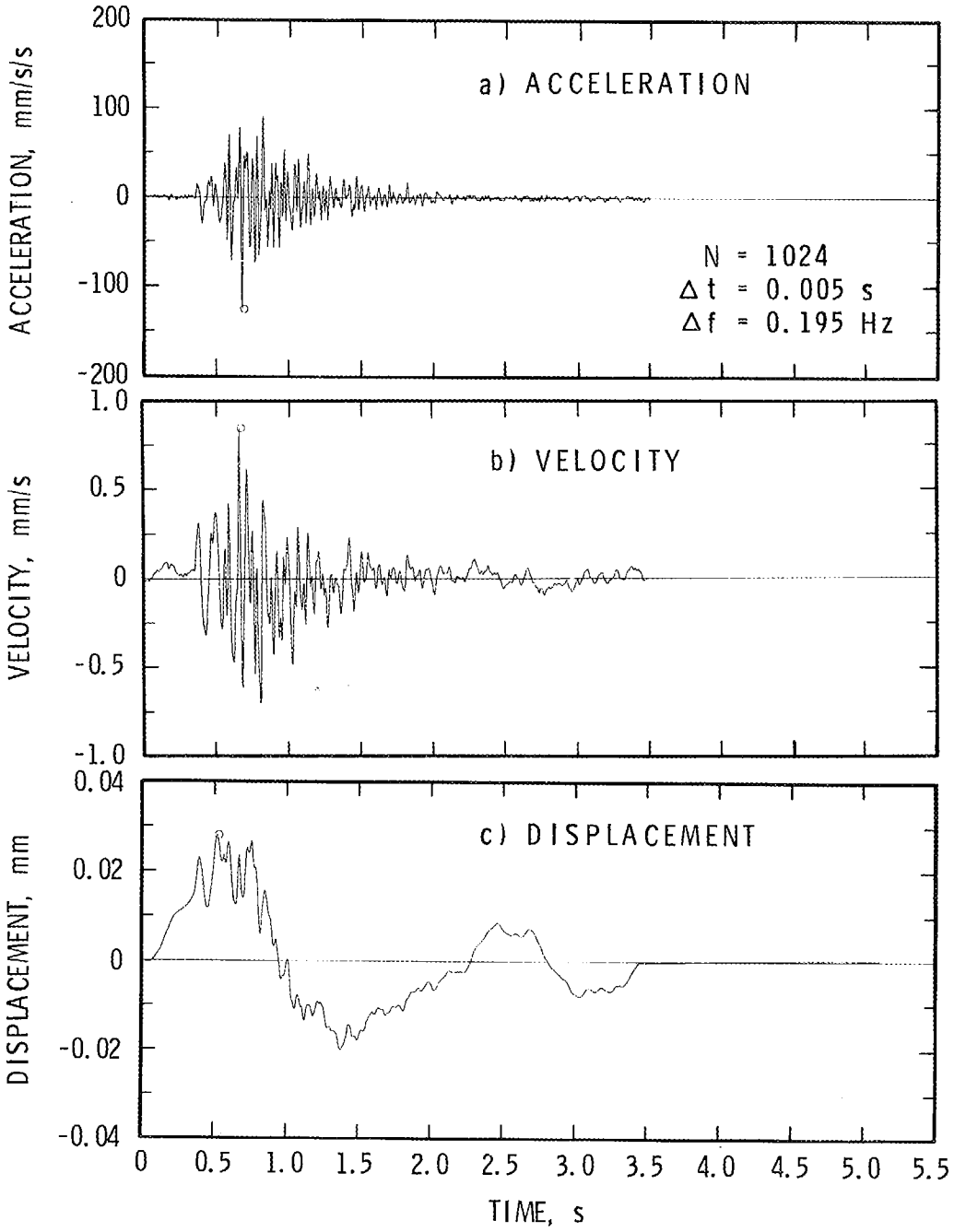

Figure 5 Acceleration record adjusted for velocity and displacement boundary conditions and resulting velocity and displacement.

effects. The example presented represents a particularly severe test of the method since the resulting displacements are extremely small, in the order of 0.03 mm.

COMPUTATIONAL CONSIDERATIONS

Sampling Frequency

The sampling frequency of a signal is governed by the following requirements. First, there must be adequate resolution so that closely-spaced frequencies can be distinguished and the frequency response curves be properly defined; this requires that the frequency increment Δf is approximately six times the half-power bandwidth of the frequency response curve for the vibration system, and for close frequency spacing, that Δf is at least six times the frequency difference to be resolved. Second, to avoid 'aliasing', the sampling frequency (f_s) needs to be at least twice the highest frequency component ($f_{\max}$) in the signal [3,4,12]. Finally, if the time record is to be represented with adequate resolution, then the sampling frequency should be at least six times, preferably ten times, the highest frequency component in the signal.

Transform of Long Records

When the number of points to be transformed exceeds the capacity of the available computer, either in storage capacity or on account of the software used, a method of sectioning the total number of points into an integer number of subarrays can be used, as is shown in Reference 13. Each of these subarrays needs to have 2^n points, since the FFT algorithm is employed there. This method also presents the possibility of transforming an array whose total number of points is not 2^n, but is an integer multiple of a smaller power of 2.

Another method of processing long records is the 'overlap–save' method, where sequential overlapping sections of the signal are processed and the overlap with the spurious results discarded. This is an approximate method, but should provide adequate accuracy for many practical problems (see Reference 14 for further details).

Wrap-Around

The discrete Fourier transform (Eq. (1)) is a circular function which can be viewed as repeating itself for succeeding portions of $2N$, $3N \ldots$ points. This means that the end of the record can be thought of as continuing at the beginning of the succeeding identical record, or equivalently, the beginning of the same record. Thus, the record has to start and end at the same value, otherwise a discontinuity results. As a consequence of this circular property, signals which result from an operation that employs the DFT (or FFT) and which have not died out before the end of the record will re-appear at the beginning, resulting in a phenomenon referred to as 'wrap-around'.

This effect is particularly important when a response calculation is carried out according to Eq. (5) with subsequent inverse Fourier transform. The calculated response of the

vibrating system has to die out to zero (or sufficiently close to zero) before the end of the calculation period of N points, otherwise the residual oscillations will re-appear at the start of the calculated signal. This requirement is satisfied by the criterion (see Ref. 14):

$$N = P + Q - 1 \tag{26}$$

where:

N = total number of points,

P = number of points in the signal,

Q = number of points of the impulse response function of the vibrating system or oscillator.

Leakage

Because the DFT encompasses only a finite length of record, any abrupt change of signal level at the beginning or end of the record causes 'leakage' of frequency components and a distortion of the Fourier transform. It is therefore necessary to start and end the record with zero values and provide reasonably gradual transitions to the signal. If the record itself is not inherently of such a type, then a time window function that accomplishes this objective needs to be applied. A time window commonly employed is the cosine taper, which can range over portions of the record duration, to a full cosine tapering over the entire record length (see Fig. 6).

The leakage properties of a time window are governed by the side lobes in the Fourier transform of the window (see Figs. 7 and 8). The larger these lobes, the more extraneous oscillations the filtered signal will display. A detailed evaluation of the cosine taper time window follows.

The cosine taper time window shown in Figure 6 is given by:

$$g(t) \quad \begin{cases} = \frac{1}{2}(1 + \cos(\frac{2\pi}{aT}[t - \frac{T}{2}(1-a)])), & \frac{T}{2}(1-a) \le t \le \frac{T}{2}, 0 \le a \le 1 \\ = 1, & -\frac{T}{2}(1-a) \le t \le \frac{T}{2}(1-a) \\ = \frac{1}{2}(1 - \cos(\frac{2\pi}{aT}[t + \frac{T}{2}])), & -\frac{T}{2} \le t \le -\frac{T}{2}(1-a) \end{cases} \tag{27}$$

and the Fourier transform can be shown to be:*

$$G(f) = \frac{\pi^2}{\omega(\pi^2 - \omega^2 a^2 (\frac{T}{2})^2)} (\sin(\frac{T\omega}{2}(1-a)) + \sin(\frac{T\omega}{2})). \tag{28}$$

* H.H. Ireland, private communication.

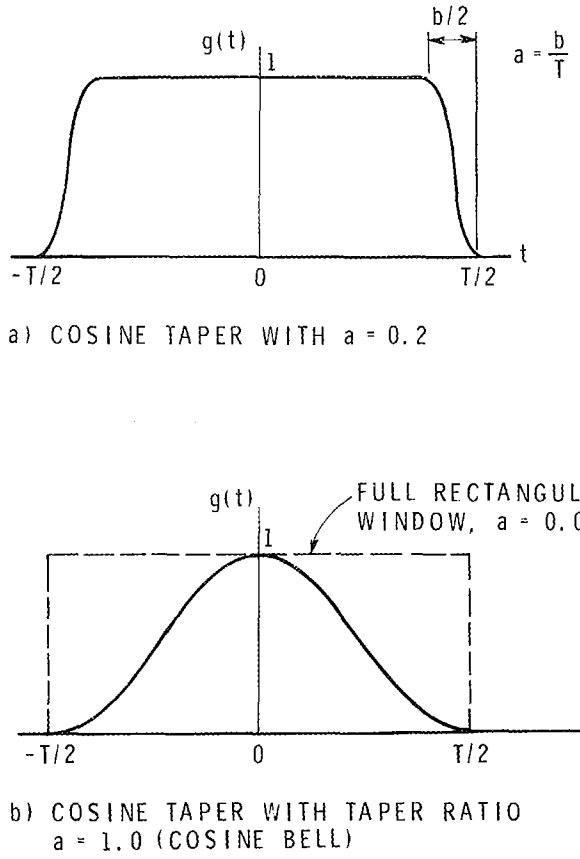

Figure 6 Cosine taper windows with various taper ratios a.

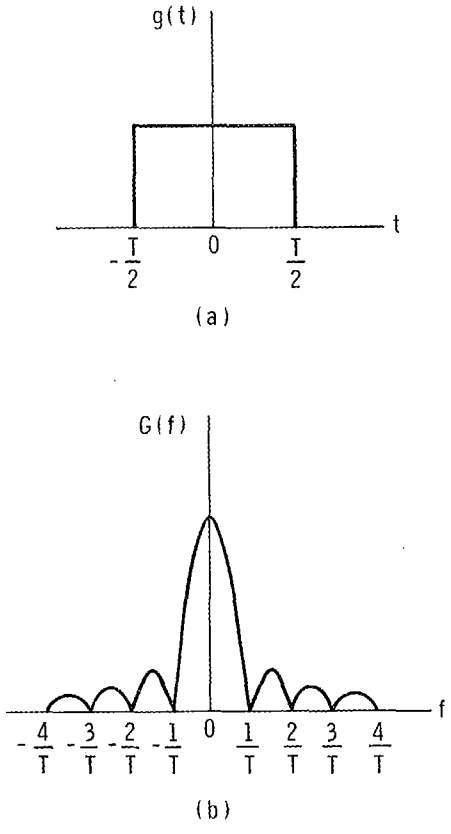

Figure 7 (a) Rectangular window (b) Fourier amplitude spectrum.

Plots of $G(f)$ are presented in Figures 8a and b. For this example, the taper ratio a was set equal to 20% of the total digitization window length of 227.555 seconds. Figure 8 shows that the Fourier transform of the cosine taper is made up of a main central lobe, to either side of which occur periodically-spaced lobes of decreasing magnitude. The first or main lobe, having an actual spectral magnitude of 204.8, has been truncated so that the side lobes can be displayed more effectively; thus Figure 8b is a continuation of Figure 8a and is further magnified in amplitude and frequency.

It is clear from Eq. (27) that as the value of the taper ratio a increases from a value close to zero towards 1.0, the cosine tapering of the beginning and end of the digitization window becomes increasingly more gradual. From an analysis of the Fourier transform of the taper cosine under the same conditions,* the first zero crossings to either side of the centre lobe take on increasing frequency values given by:

$$f_{\text{zero crossings}} = \frac{2}{(2-a)T}. \tag{29}$$

* H.H. Ireland, private communication.

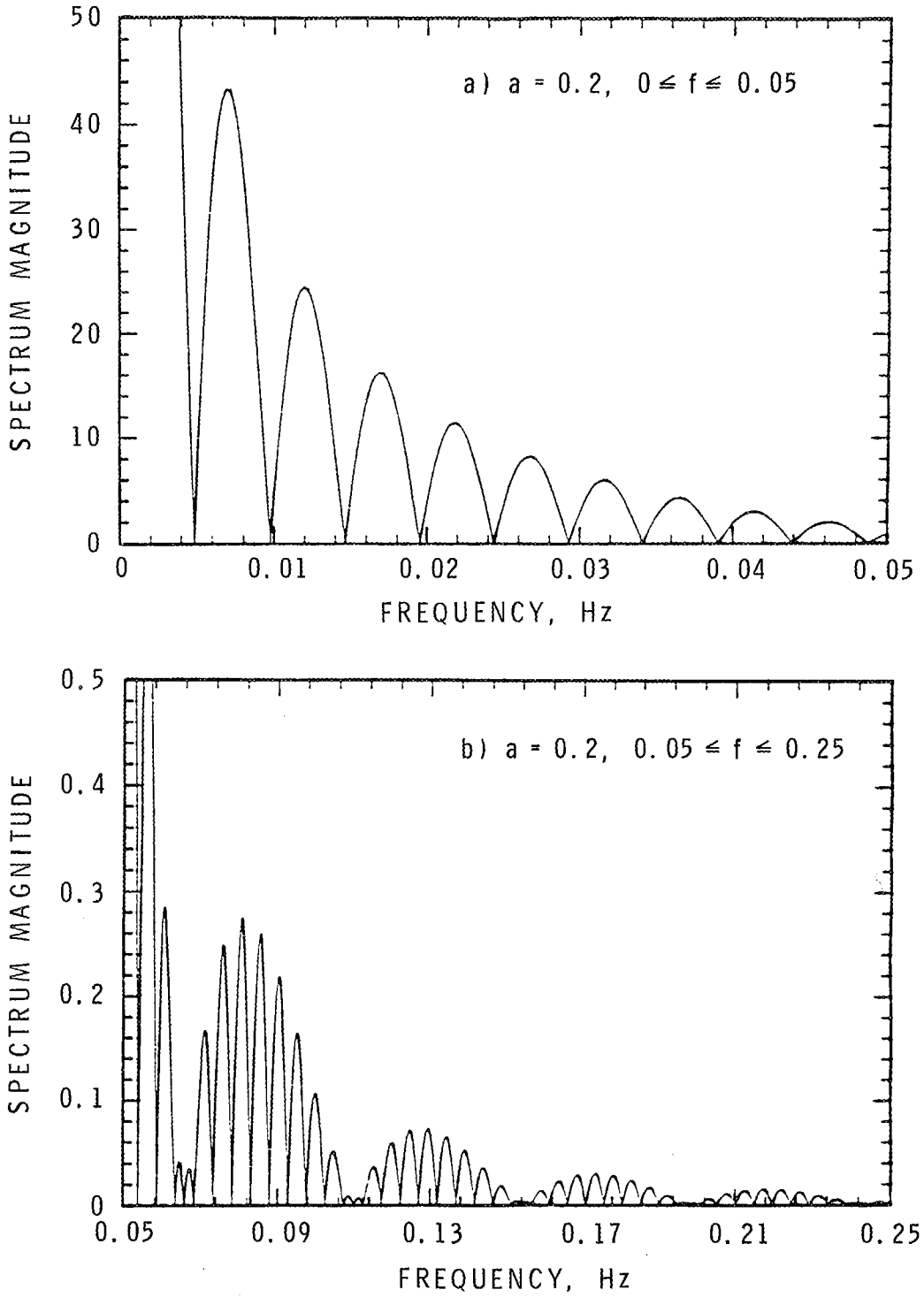

Figure 8 Cosine taper Fourier transform.

Furthermore, Eq. (29) shows that the centre lobe is spread over a larger bandwidth as a increases. At the same time, the magnitude of this centre lobe decreases for increasing values of a according to:

$$| G(f_c) | = \frac{T}{2} - \frac{T}{2}(1 - a). \tag{30}$$

In qualitative terms, as the taper ratio a is decreased, or equivalently, as the shape of the window becomes increasingly rectangular, the magnitude of the centre lobe increases and its bandwidth decreases, with a simultaneous increase in the magnitude of the side lobes. Therefore, a decreased taper ratio increases the amount of leakage. Conversely, as the taper ratio is increased or the window shape becomes more like that of a 'cosine bell' (Fig. 6b), the main lobe becomes lower, its bandwidth increases, and the magnitude of the side lobes decreases. The effect of this decrease in a is to reduce the amount of leakage but it gives rise to a decrease in the resolution of closely-spaced spectral components since the width of the centre lobe increases.

An increase in a also decreases the centre amplitudes of the resulting Fourier spectrum $G(f_c)$ according to Eq. (30) for cases where the signal energy is uniformly distributed over the duration T. For a full cosine bell (i.e., $a = 1.0$), the spectral amplitudes will then be half of the non-windowed case. This also corresponds to the area reduction of the full cosine taper relative to the full rectangular window.

In order to deal with the leakage effects, the following are indicated:

1) a time window function with side lobes as small as possible should be chosen, which means a window function having gradual slopes;
2) the number of points in the time record at the beginning and end should be augmented with zeros, so that the effects of leakage occurring in these portions can be assessed and subsequently discarded.

Illustrative Examples of Leakage

The effects of leakage are illustrated for various time windows applied to a record arising from floor vibrations due to a coordinated activity. The full time record and its Fourier transform are shown in Figures 9a and b. The record is composed of three main frequency components, and the time trace indicates a slight start-up phase. In order to illustrate the leakage effects and to deal with a more constant signal, the first two seconds are zeroed (three seconds for the boxcar filter). After 'windowing' the time record, the Fourier transform is computed and multiplied by a frequency cosine taper window with $f_1 = 0.2$, $f_2 = 1.0$, $f_3 = 2.5$ and $f_4 = 3.0$ Hz - hereafter designated by the array of the type (0.2, 1.0, 2.5, 3.0 Hz). (See Figure 1 for a definition of the filter frequencies f_1 to f_4). Then the inverse Fourier transform is computed. The total operation effectively produces a bandpass filter around the lowest frequency component at 2.36 Hz. Since this frequency window truncates the transform in a region of very low signal energy, the effects of leakage

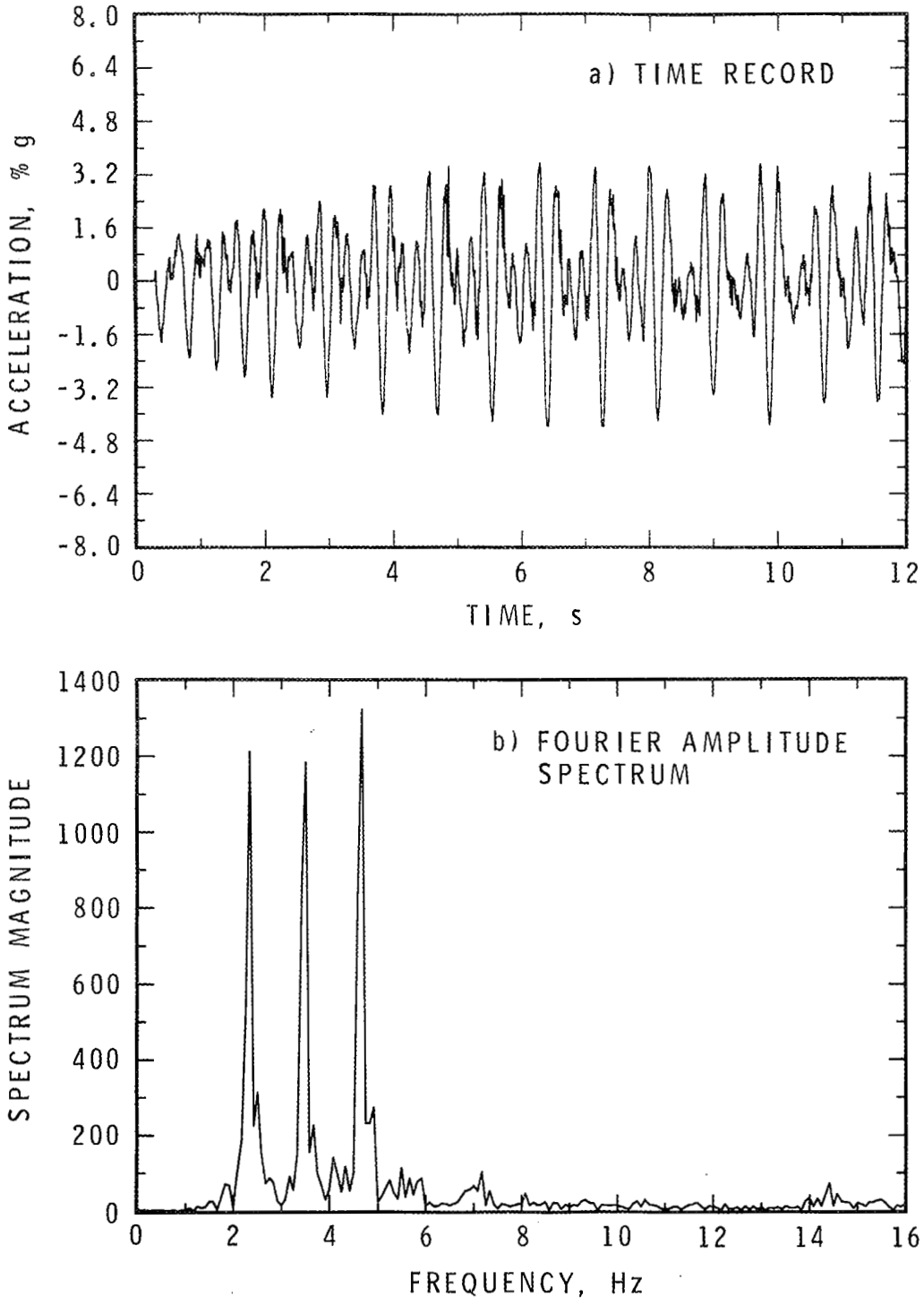

Figure 9 Record of floor vibrations from coordinated activity.

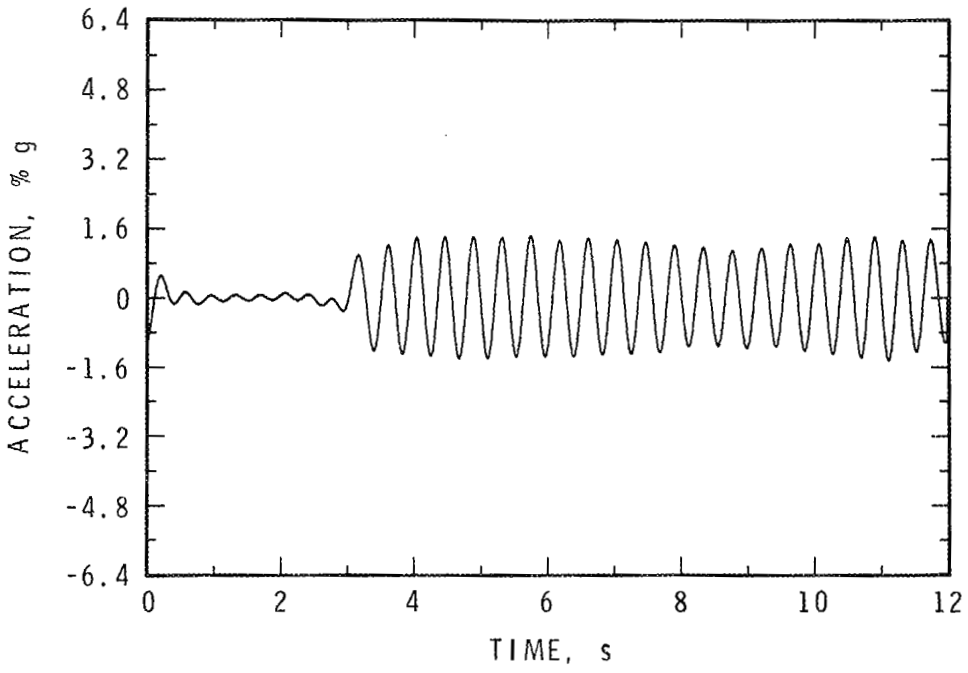

Figure 10 Filtered time record with rectangular time window (boxcar) from 3 to 12 s.

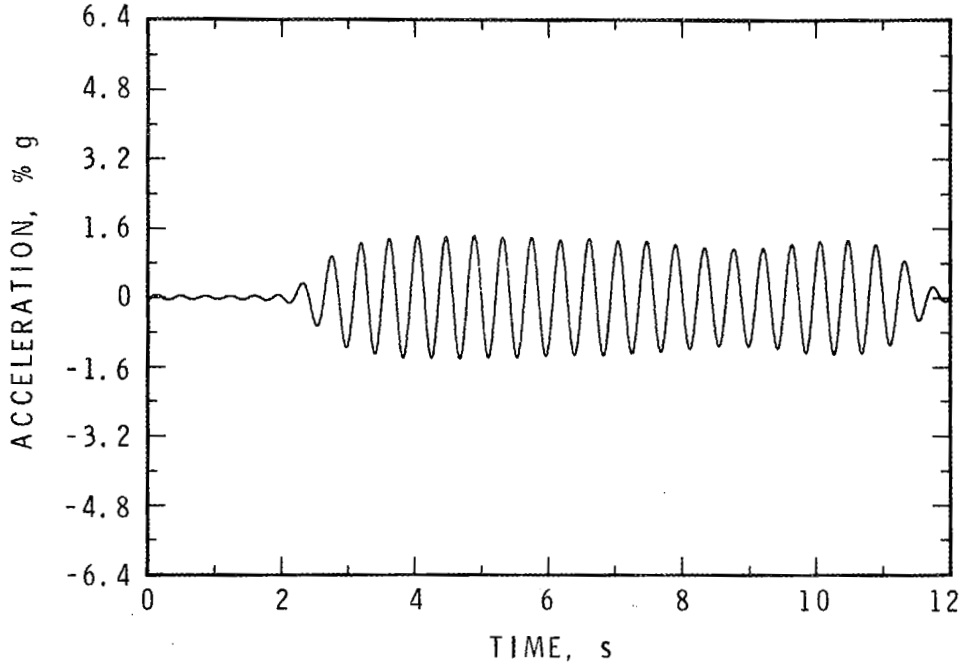

Figure 11 Filtered time record with tapered cosine time window, $a = 0.2$.

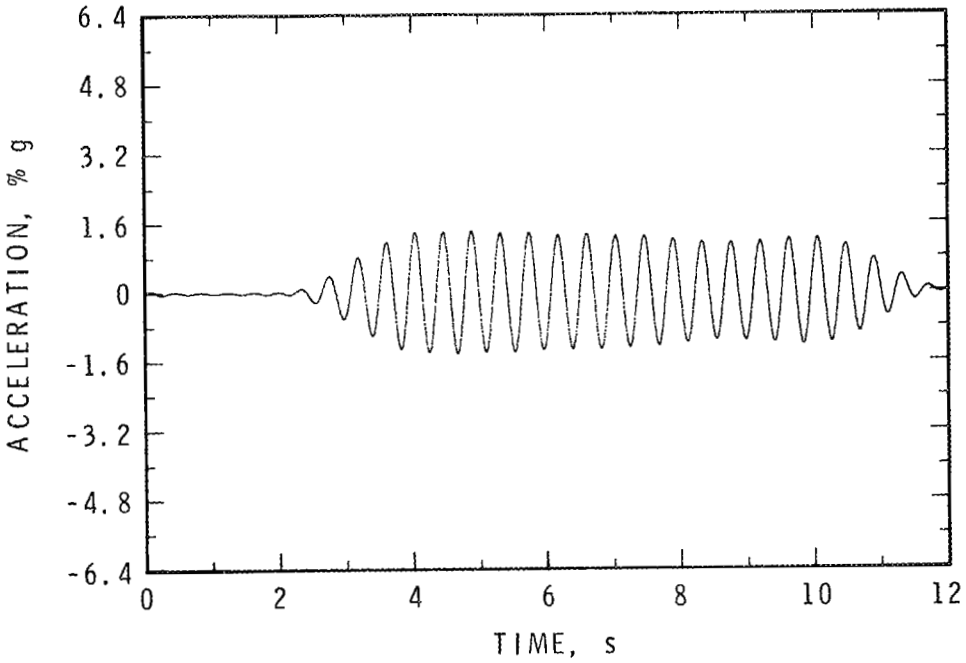

Figure 12 Filtered time record with tapered cosine time window, $a = 0.4$.

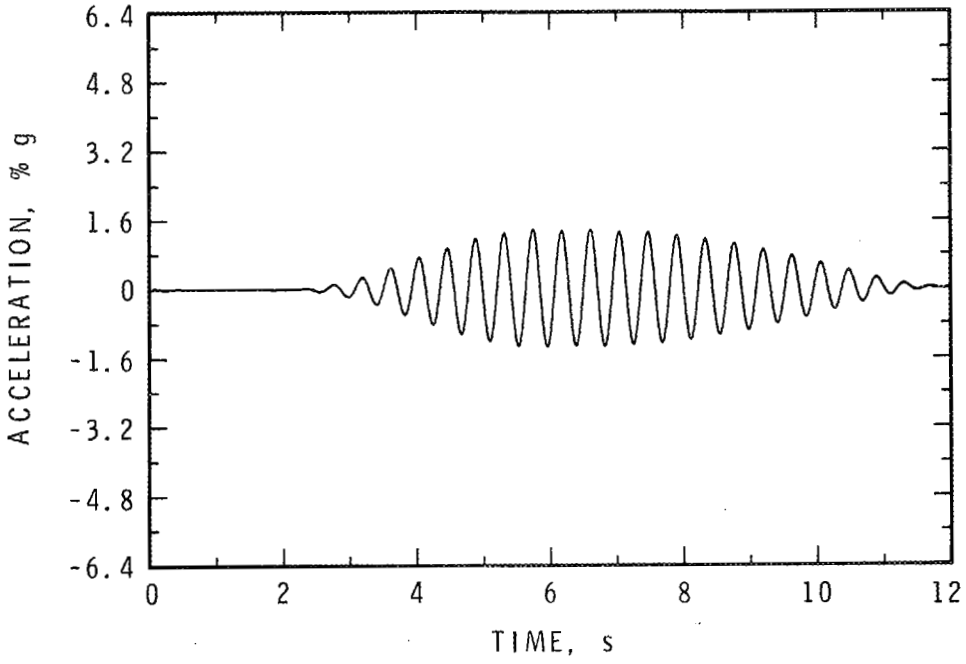

Figure 13 Filtered time record with tapered cosine time window, $a = 0.8$.

from a frequency window will be negligible. The same frequency window is used for all subsequent examples.

The results of filtering using various time windows are shown in Figures 10 to 14. Starting with the boxcar time window in Figure 10, to increasing values of the cosine taper ratio a in Figures 11, 12 and 13, the spurious oscillations before the start of the signal decrease steadily, until for the (2, 6, 8, 12 second) taper window there is virtually no residual signal, meaning virtually no leakage. Within the transition zone, the signal amplitudes are of course reduced due to the time window taper. However, significant portions of the signal in these zones could be recovered by dividing by the corresponding taper amplitudes. Away from the taper zones, the signal amplitudes are virtually indistinguishable among the various window functions.

Another window function that can be used is the trapezoidal one. The results for the (2, 4, 10, 12 second) window are shown in Figure 14. The extraneous oscillations in the quiescent portion of the signal are virtually identical to the results shown in Figure 12, obtained from the time domain cosine taper window with $f_1 = 2$, $f_2 = 4$, $f_3 = 10$, $f_4 = 12$ seconds, or $a = 0.4$.

Further theoretical treatment of this topic can be found in References 4, 12, 15 and 16.

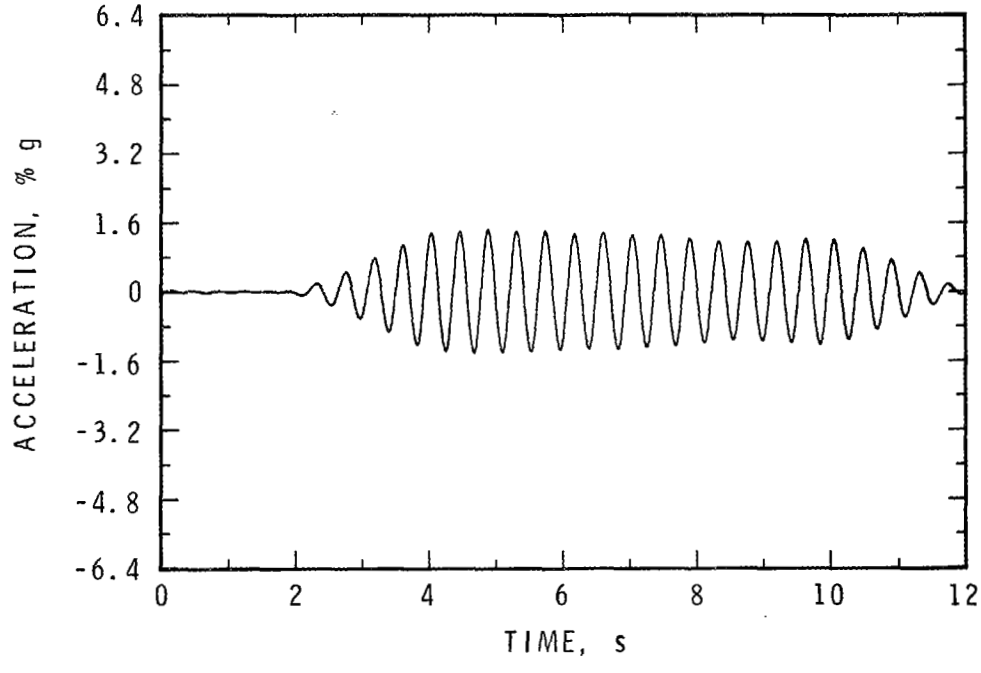

Figure 14 Filtered time record with trapezoidal time window, $a = 0.4$.

CONCLUSION

The Discrete Fourier Transform computational method has been shown to be useful for processing vibration signals to achieve instrument correction, integration, differentiation, baseline adjustment, and filtering. However, aspects of aliasing, leakage and wrap-around need to be considered.

ACKNOWLEDGEMENT

The mathematical results for the cosine taper window were obtained by H.H. Ireland during the cooperative work term in the winter of 1984–85 in the Noise and Vibration Section of the Institute for Research in Construction. The assistance of W. Mlacak, L. Belisle, and H.H. Ireland in developing various portions of computer programs employed in the analyses, and the assistance and discussions of colleagues in the Noise and Vibration Section are gratefully acknowledged.

REFERENCES

1. Brigham, E.O. *The Fast Fourier Transform.* Prentice-Hall Inc., Englewood Cliffs, N.J., 1974, 252 p.

2. Jenkins, G.M. and Watts, D.G. *Spectral Analysis and Its Applications.* Holden-Day, San Francisco, 1968, 525 p.

3. Bendat, J.S. and Piersol, A.G. *Measurement and Analysis of Random Data.* John Wiley & Sons Inc., N.Y., 1966, 388 p.

4. Oppenheim, A.V. and Shafer, R.W. *Digital Signal Processing.* Prentice-Hall Inc., Englewood Cliffs, N.J., 1975, 585 p.

5. Rainer, J.H. Dynamic Response by Fourier Transform. DBR Computer Program 29, Division of Building Research, National Research Council Canada, Ottawa, 1970.

6. Bergman, G.D. A Guided Tour of the Fast Fourier Transform, IEEE Spectrum, Vol. 6, p. 41-52, 1969.

7. Rainer, J.H. Effect of Rotation on Motion Measurements of Towers and Chimneys. Building Research Note 230, Division of Building Research, National Research Council Canada, Ottawa, 1985.

8. Rainer, J.H. Rotation Effects on Measurements of Lateral Motion. In press, Earthquake Eng. and Struct. Dyn., 1986.

9. Trifunac, M.D. and Lee, V.W. Routine Computer Processing of Strong-Motion Accelerograms. California Institute of Technology, Earthquake Engineering Research Laboratory Report No. EERL 73-03, Pasadena, CA, 1973.

10. Kausel, E. and Ushijima, R. Baseline Correction of Earthquake Records in the Frequency Domain. Dept. of Civil Engineering, M.I.T., Cambridge, Mass., Public. No. R79-34, 77 p., 1979.

11. Anderson, J.G. Two Observations About Low-Frequency Signals on Accelerograms From the October 15, 1979 Imperial Valley, California Earthquake. Earthquake Eng. and Struct. Dyn., Vol. 13, p. 97-108, 1985.

12. Bendat, J.S. and Piersol, A.G. *Engineering Applications of Correlation and Spectral Analysis.* John Wiley & Sons, N.Y., 1980, 302 p.

13. Chu, W.T. A Technique for Zoom Transform and Long-Time Signal Analysis. Canadian Acoustics, Vol. 11(3), 1983, p. 45-50.

14. Chinoy, C.B. and Lewis, P.T. Acoustical Signal Processing: FFT Convolution and Deconvolution. Acoustics Letters, Vol. 8(8), p. 120-127, 1985.

15. Thompson, J.K. and Tree, D.R. Leakage Error in Fast Fourier Analysis. J. Sound and Vibration, Vol. 71(4), p.531-544, 1980.

16. Harris, F.J. On the Use of Windows for Harmonic Analysis with the Discrete Fourier Transform, Proceedings of the IEEE, Vol. 66(1), p. 51-83, 1978.